ELSEVIER

Journal of Nuclear Materials 270 (1999) 134–146

journal of nuclear materials

A hydrogen uptake micro-mechanism for Zr alloys

B. Cox *, Y.-M. Wong

Centre for Nuclear Engineering, University of Toronto, 184 College Street, ON Toronto, Canada M5S 3E4

Received 30 April 1998; accepted 19 October 1998

Abstract

Past attempts to develop a micro-mechanistic model for the hydrogen uptake process during zirconium oxidation have concentrated on solid state diffusion through a barrier oxide. Experimental results have often been invalidated by artefacts. Recently it has become evident that the uptake may be via flaws in the oxide film which penetrate, at least briefly, up to the metal–oxide interface. An attempt to characterise and locate such flaws in oxide films on specimens from a number of batches of several zirconium alloys is reported here, using cathodic polarization to deposit small Cu balls on the active cathodic sites and scanning electron microscopy to identify and characterize these sites. In oxides on Zircaloy-2 samples, the cathodic sites were usually small cracks in the oxide, sometimes (but not always) at pits where intermetallic particles had been etched out during the initial surface preparation. The same cathodic sites could be decorated during successive cathodic polarizations, but even a short subsequent oxidation (1 day, 400°C steam) re-passivated all previous sites, and created new ones. In one batch of Zr–2.5%Nb alloy, that contained an array of large carbides, cracks in the oxide at the sites of these particles provided the cathodic sites. In the absence of such particles, far fewer cathodic sites were found in oxides on Zr–2.5%Nb alloy specimens than on Zircaloy-2 specimens. These few sites were always small cracks in the oxide film. Exposure to a low pressure hydrogen atmosphere created many more cracks and cathodic sites in the oxide on Zr–2.5%Nb.

1. Introduction

The observation that zirconium alloys absorbed some hydrogen during corrosion in water was one of the earliest consequences of the oxidation process in high-temperature water to be established [1]. Forty-five years later, the large amounts of hydrogen absorbed by Zircaloy-4 cladding in pressurized water reactors after high fuel burnups have become one of the factors limiting the achievable lifetime for the fuel [2,3]. Redistribution of this hydrogen as a result of small local temperature gradients (e.g. at pellet interfaces or spalled oxide patches) has been one of the contributing factors here [4–6] because of the concern that such areas might be very brittle. Hypotheses for the mechanism involved in this hydrogen absorption process have been proposed at regular intervals during the intervening years, yet without any clear agreement being reached on the micro-mechanism involved.

For much of this time there has been a tendency to regard the mechanisms for hydrogen absorption from hydrogen gas by preoxidised specimens and the mechanisms by which hydrogen enters the metal during corrosion in aqueous environments as being basically different [7,8]. Recent publications [9,10] have concluded, however, that the hydrogen uptake process during aqueous corrosion is very localised, and that there may be little difference (except of scale) between uptake from hydrogen gas and from aqueous environments. It is the purpose of this paper to present the results of current studies aimed at identifying the localized sites at which hydrogen may be being absorbed and to characterize their persistence (or otherwise) during oxidation. However, it would appear to be valuable to first look at the previous hypotheses for hydrogen uptake to see why they fail to explain the observed phenomena.

* Corresponding author. Tel.: +1-416 978 2127; fax: +1-416 978 4155; e-mail: cox@ecf.utoronto.ca

0022-3115/99/$ – see front matter
PII: S0022-3115(98)00898-8

2. Past hypotheses

It was assumed, to begin with, that (at least during pre-transition oxidation), oxide growth and hydrogen absorption both proceeded completely by solid state diffusion processes, even in high temperature water. Furthermore, it was argued that the diffusion coefficients for hydrogen in zirconium oxide films could be measured by exposing preoxidized specimens to a low pressure of hydrogen gas [11–14]. This was maintained despite the long-published observations that the oxide on zirconium underwent a rapid breakdown (in <5 min. at 400°C) if the specimens were transferred from an oxygen to a hydrogen atmosphere [15–17] and that during such exposures (in hydrogen or in vacuo) some dissolution of the oxide into the metal occurred [18].

Despite the evidence that some sort of sudden breakdown in the oxide was necessary before rapid uptake of hydrogen gas ensued, the onset of this rapid uptake was correlated with an increase in the oxide conductivity during the exposure of preoxidized specimens to vacuum or hydrogen, which was explained as to be indicative of an increase in the vacancy concentration in the oxide. The enhanced diffusion of some hydrogen species as a result of the enhanced vacancy concentration was proposed as the mechanism of hydrogen ingress [11–14]. Later work in this field correctly established that the uptake process was phase boundary controlled and not diffusion controlled after oxide breakdown [19].

During the course of these studies, it became evident that, at temperatures below ~600°C (873 K) the diffusion of the oxide film into the metal was highly localized at grain boundaries [20,21]. This suggested that, in order to evaluate the nature of the breakdown process leading to the rapid uptake of hydrogen gas, it would be necessary to do some high resolution electron microscopy on the prior metal grain boundary regions of thin oxide films before and after exposure to vacuum or hydrogen. When studies of this type were performed on van Arkel zirconium [7], it was observed that rapid dissolution of the oxide films occurred at preferred sites along the prior metal grain boundaries and generated small pores that passed right through the oxide film. The average oxide thickness did not change significantly during this pore generation at temperatures $\leqslant$400°C (673 K). This explanation fitted the observations of rapid hydrogen uptake following an incubation period for exposures to hydrogen gas, but was not believed to be possible in the presence of an oxidizing atmosphere, since even small additions of oxygen were found to stop uptake from hydrogen gas [22,23].

Nevertheless, some investigators still think that the rates of transport of hydrogen through oxide films that are measured by exposing preoxidized specimens to low pressure hydrogen atmospheres represent the diffusion of hydrogen through the ZrO_2 of the oxide film, or through some fraction of its thickness described as the 'barrier film' [24,25], since they equate their results either with 'effective diffusion coefficients' or associate them with earlier claims to have been measuring such a diffusion coefficient [14]. The correct interpretation of the hydrogen or deuterium profiles measured by secondary ion mass spectrometry (SIMS) in such studies, however, requires considerably more information than was provided. Not least, the question of whether hydrogen species observed in oxide films are in fact in transit into the metal substrate must be addressed. An answer to this question for preformed oxide films exposed to hydrogen gas was given early [26] by tritium autoradiography studies which showed that exposures to gaseous tritium revealed tritium in the metal phase but no tritium in the oxide through which it had passed. This is in line with the explanation given above for exposures of preoxidized specimens to hydrogen, and suggests that the hydrogen species observed in oxide films grown in aqueous environments are not those involved in the hydrogen uptake by the metal. They are either species incorporated in pre-transition oxides during the corrosion process (which are immobile) or OH^- groups on the walls of pores in porous oxides (which are rapidly exchanged).

Early nuclear reaction results showed that the average hydrogen (deuterium) concentration in a thin oxide film is about ten times greater than that in the metal [27]. This has been confirmed by conventional analytical techniques for thick oxide films formed in-reactor [28]. By comparing analytical results for autoclave specimens with and without their oxides removed [29] it was found that the hydrogen concentrations in the oxide and the metal were similar (Table 1) during laboratory testing.

Recent studies have shown that H can be exchanged for D (and the reverse) in an oxide film on an almost quantitative basis without any evidence that a different fraction of these species entered the metal than would have been normal for the time and temperature of the exchange experiment. This exchange can be made quickly (a fraction of an hour) at temperatures around 300°C (573 K), and at similar speeds for the $Li^{6/7}$ and $B^{10/11}$ exchange processes if these species had been incorporated into the oxide by exposure to solutions containing LiOH or H_3BO_3 [30,31]. That all three exchange reactions should proceed at similar rates is plausible only if the species are in similar locations in the oxide. This will most probably be the case if all three species are present as ions adsorbed on pore walls in the oxide. The profiles of each species would then indicate the distribution of porosity in the oxide rather than a diffusion profile in the ZrO_2 lattice.

There is still no satisfactory value for the diffusion coefficient of hydrogen species in the ZrO_2 lattice. Some preliminary nuclear magnetic resonance experiments on deuterium in oxide films suggested very low jump frequencies and hence diffusion coefficients, but the study

Table 1
Hydrogen contents measured in ZrO_2 films formed in pH 12 LiOH at 360°C.

Specimen numbers	Over pressure	Δw (mg/dm^2)	Initial H (ppm)	Final H (ppm)			H in oxide (ppm) (estimated)
				Oxide present		Oxide removed	
				150°C degas	350°C degas		
A4	H_2	351	14	906	841	883	565–885
A8	O_2	357	14	1096	1088	1150	690–735
B4	H_2	520	16	836	831	944	455–475
B8	O_2	499	16	1283	1401	1319	1030–1065
C4	H_2	579	15	5474	6735	6544	2400–6300
C8	O_2	445	15	3933	4325	4783	865–2390
7-3	O_2	222	7	715	739	698	1790–2030
8-4	O_2	304	10	639	628	634	505–590

was not completed. Attempts to measure diffusion coefficients using deuterium implanted into oxide films on Zr–Nb alloys and Zircaloy-2 [32,33] showed loss of deuterium during the implantation process and decreasing peak heights without peak broadening following short anneals in air. No examination of the oxides for radiation damage as a result of the implantation was performed. The attempt to avoid oxide breakdown by performing the anneals in air was probably inappropriate for Zr–Nb alloys as it has long been known that transfer of Zr–Nb alloys oxidized in steam to an oxygen containing environment results in a rapid oxide breakdown [34,35]. This was thought to result from microcracking resulting from the oxidation of NbO_2 (the highest niobium oxide formed in steam) to Nb_2O_5, with a correspondingly large increase in volume. Preliminary observations [36] of the location of Nb in the oxide on the α-Zr phase of Zr–2.5%Nb have shown the existence of isolated high Nb oxide crystallites amongst the predominantly low Nb crystallites of ZrO_2, forming the majority of the oxide on the α-Zr areas. Oxidized β-Zr regions with their high Nb contents also show high Nb in the oxide but the crystallite size is too small to distinguish the individual crystallites [36,50].

One of the early observations of variability in hydrogen uptake between alloys showed a strong dependence on the chemical nature of the alloying additions, most of which were relatively insoluble in zirconium, and hence were present in the form of intermetallic particles [37,38]. The very different hydrogen storage properties of these intermetallics when compared to the zirconium matrix led to the suggestion that intermetallic particles in the oxide/metal interface might act as 'windows' for hydrogen entry [7,39]. This has led to several recent studies where hydrogen concentrations in the intermetallic particles have been observed by tritium autoradiography [40–42]. Such evidence has been argued to favour an ingress route via the intermetallics for hydrogen absorbed during aqueous corrosion. However, the difference in the heats of solution and solubilities for hydrogen in the intermetallics phases compared with the matrix suggests that these redistributions into the intermetallics occur during the cooling of the specimens. This is the same property difference that leads to hydrogen segregation into the Zr barrier in barrier cladding during cooling [43]. Whether a fast enough quench could be performed on the intermetallics to show whether the hydrogen was concentrated in them during corrosion has not yet been demonstrated.

Nevertheless, experiments in which Zircaloy-2 still showed higher initial hydrogen uptake rates than Zircaloy-4, even though all Zr_2(Fe/Ni) particles in the surface had been dissolved during the initial pickling of the specimens, suggested that the intermetallic particles themselves were not participating directly in the hydrogen uptake process [10]. If the ingress is via small flaws in the oxide as was proposed, then it would be the effect of the intermetallics (or the geometrical effects of the etch pits resulting from their dissolution) on the local flaw generation process that would be the important factor.

The aim of this study has been to identify the locations of the cathodic sites (the points at which the cathodic half-cell reaction proceeds during oxidation) in a range of alloys and batches to establish what the common features of such sites are, and to see whether such sites are permanent features of the oxide or change randomly as oxidation progresses.

3. Experimental

Specimens were selected from already oxidized coupons for which the corrosion conditions were well known. Samples came from batches of van Arkel zirconium (Be), Zircaloy-2 (Bh) and Zr–2.5%Nb (U, Bg, Aw and pressure tube#790). Details of the specimens are given in Table 2, and analyses of the materials in Table 3.

The specimen edges were masked with epoxy, and other anomalous features (e.g. any scratches received

after oxidation) were also masked. The specimens had a small electrical contact abraded in one corner and were then cathodically polarized in 0.1 molar $CuSO_4$ under conditions established previously [44] for depositing small copper balls at sites where the cathodic current was flowing in anodic oxide films. Maximum voltage and current were limited to 2 V and 1 mA/cm^2, respectively, to avoid potential damage to the oxide. For instance, in some samples where only one or two active cathodic sites were observed per mm^2 there was a concern that ohmic heating at these sites might cause oxide breakdown. After copper deposition, the location of the copper deposits was mapped using a SEM. The copper deposits were then dissolved in 50% nitric acid and the deposition sites were revisited to identify the features at which the cathodic current had flowed.

The copper deposition process was repeated at least once more on all specimens to establish whether the same sites were still active, and to ensure that no new sites had been created. After the final deposits had been removed, the epoxy was also removed and the specimen surface cleaned. Specimens that had initially been oxidized in 400°C steam were then reoxidized under the same conditions and the copper deposition process repeated to see if the same sites remained active.

4. Results

Copper deposits were formed invariably at small cracks in the oxide film on Zircaloy-2, even for pretransition oxide (~1.2 μm). These cracks were typically at either the sites of residual scratches in the initial surface (Fig. 1), where residual stresses in the metal led to an array of cracks, or at small cracks around the edges of etch pits resulting from the dissolution of intermetallic particles during specimen preparation (Fig. 2). These active cathodic sites remained in operation when the copper deposition and removal step was repeated (Fig. 3). The sizes of the Cu balls deposited on the various active sites changed considerably from one deposition sequence to the next. Where there were many cathodic sites, some would not develop Cu deposits every time, but no new sites occurred after the first deposition step. The oxide film on the van Arkel zirconium specimens was very heavily cracked, especially for the thicker of the two oxide film areas (21 μm). The active cathodic sites again were cracks in the oxide (Fig. 4) generally associated with the big variations in oxide thickness found in this material [45].

Active sites on oxide films on all Zr–2.5%Nb alloy batches (except U) were fewer in number (per unit area) than on Zircaloy-2, irrespective of the oxide thickness. Sometimes only one major site was present on an area of the specimen of several mm^2 (Fig. 5). It was thought that such a single active site might be carrying all the current and preventing the overpotential for Cu deposition being reached at other sites. This was found to be the case when the large active site in Fig. 5 was masked with a small blob of epoxy. A number of minor sites then showed up (Fig. 6), although the number remained fewer per unit area than on the Zircaloy specimens. These sites were also found to be small cracks in the oxide. Because of the nature of these sites, a high current flow does not start immediately when the current is turned on after immersing the specimen in the electrolyte. The electrolyte first has to diffuse down the crack to establish a conduction path. This is shown by the slow increase of the current with time until the curve tends to a plateau (Fig. 7). In practice, since the cathodic current generates the available H by discharging protons, the most active sites would be expected to be where the most hydrogen was absorbed.

One batch of Zr–2.5%Nb alloy (U) showed many more active sites than the others. These were at sites peculiar to this batch, where a small area of thinner (<2 μm), heavily cracked oxide was observed (Fig. 8). The oxide in these areas also appeared to have been very

Table 2
Details of specimens selected for cathodic polarization

Alloy	Specimen	Oxidation temp.	Time (days)	Environment	Wt. gain (mg/dm^2)	FTIR oxide thickness (μm)		
						spot a	spot b	spot c
Zircaloy-2	Bh14	400°C	1	1 atm. steam	[1]	1.03	1.06	1.55
Zirconium	Be5	400°C	8.5	1 atm. steam	237	20.8	13.4	
Zr–2.5%Nb	Aw265	300°C	7.0	air	150			
			+0.82	air	9.0	12.3	12.0	12.7
	Bg192	300°C	7.7	air	312		17.9[2]	
	U16	300°C	2	air	54	4.2	4.3	4.2
	143A(PT#790)	400°C	1	1 atm. steam				
		+380°C	+1.5	D_2			1.57[2]	
	C1(PT#790)	400°C	1	1 atm. steam			1.54[2]	

[1]Initial weight gain unknown, additional one day oxidation, weight gain = 6.8 mg/dm^2.
[2]Average of 10 spots.

Table 3
Analysis of batches of zirconium alloys

Designation	Be	Bh	U	Bg	Aw	Pt#3790
Alloy (ppm)[1]	Van Arkel Zr	Zircaloy-2	Zr–2.5%Nb			
Sn	<10	1.45%	60	–	<10	<25
Fe	80	1400	300	840	960	565
Cr	20	900	<30	115	25	<80
Ni	<10	500	<25	13	40	<35
Nb	<100	–	2.55%	2.52%	2.70%	2.66
C	35	80	218	140	65	136
N	12	20	65	57	24	31
O	<5	1000	1220	950	1050	1150
H	2	10	45	8	4	<6
Si	<40	70	<30	57	94	61

[1]Unless otherwise stated.

porous. These sites were identified as large carbide particles (~10 μm), and much thinner oxides had formed on these particles than on the adjacent matrix (~4 μm).

The pressure tube specimens that had been oxidised in steam also showed a few active cathodic sites that were again found to be at small cracks. However, one specimen that was heated in a low pressure hydrogen atmosphere (360 h at 380°C in 10^{-3} Pa D_2) showed many more such sites. These sites clustered in groups and had a symmetry that suggested some relation to the underlying metal structure (Fig. 9). These features may be the boundaries of large α-Zr grains in the tube microstructure, but the actual sites of copper deposition were again the tips of small cracks in the oxide.

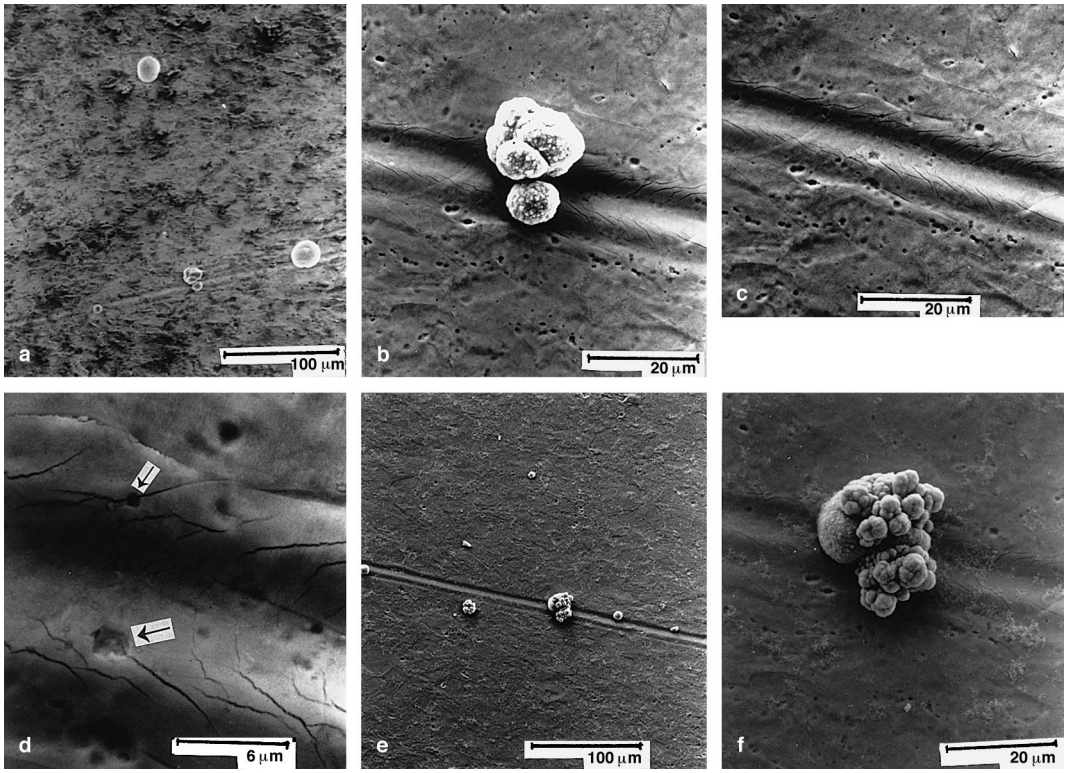

Fig. 1. Distribution and sites of Cu deposition on Zircaloy-2 (Bh14): (a) Low magnification view of Cu deposits. b) One Cu particle from (a). c) Site of Cu particle from (b) after dissolution. (d) Enlarged view of this site. (e) Repeat Cu deposition in area in (a). (f) Enlarged view of second deposition on site in (b). Arrows indicate Cu deposition sites.

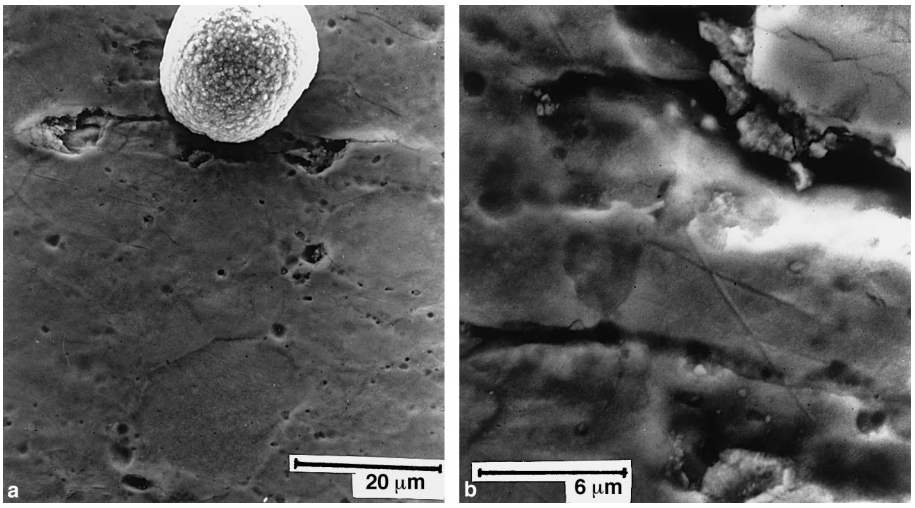

Fig. 2. Cu deposition at an array of etch pits in the original specimen surface (Bh14): (a) Cu deposit in situ. (b) Site after dissolution of Cu.

After a further 24 h in 400°C steam, none of the previous cathodic sites remained active on any of the specimens, and new sets of sites were observed (Fig. 10). Reexamination of the previous sites, now no longer active, showed that there had sometimes been some small changes in the oxide topography. These, typically, were the spalling of small pieces of oxide from the edges of prior cracks in the oxide. Where previously active sites had been at the tips of arrays of small cracks formed in the oxide on residual scratches from the specimen surface preparation, there was often no visible change in the site; not even a small extension of the crack tip could be detected (Fig. 11). Nevertheless, these sites had obviously quickly repassivated.

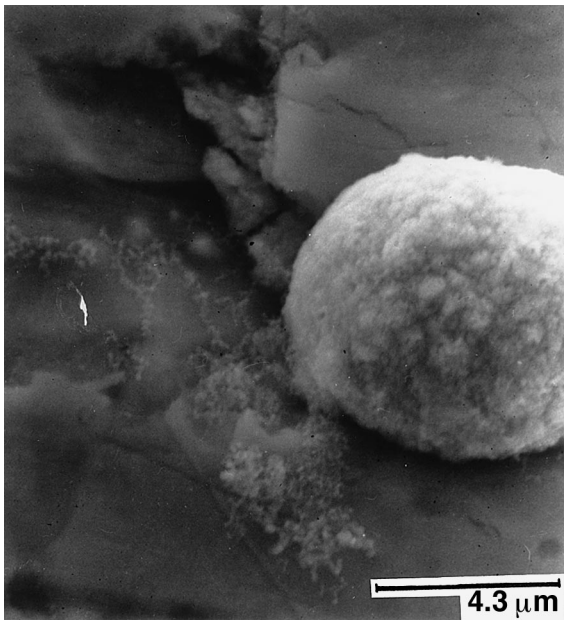

Fig. 3. High mag. view of repeat Cu deposition on the same site as Fig. 2. Note that although location was reproducible, size of Cu deposit was not.

5. Discussion

The observation that the active cathodic sites, in almost all cases, were found to be at the tips of small cracks visible in the oxide surface (Figs. 1(d) and 5(c)), and that the cathodic current required some time to reach equilibrium after the start of polarisation (Fig. 7), supports the hypothesis, presented earlier [9,10], that hydrogen uptake takes place at sites where the oxide–metal interface is directly accessible to the environment at least for a brief period after the formation of the crack or pore. Furthermore, the repassivation of these sites and the generation of new ones supports the argument that uptake sites are active only briefly during oxidation, and any barrier layer is only a time-averaged boundary marking the locus of the points of nearest approach of cracks or pores to the oxide–metal interface [8]. It was not possible with this technique to establish precisely what the sites looked like at the oxide–metal interface, but they probably look much like they do on the surface since the sites identified in thin (80 nm) anodic films had the same appearance [44].

The results also support the position that, at any moment in time, a few of these flaws will pass right through the oxide films. This argument was first made for post-transition films on the basis of the effect of pressure-changes made during oxidation on the instan-

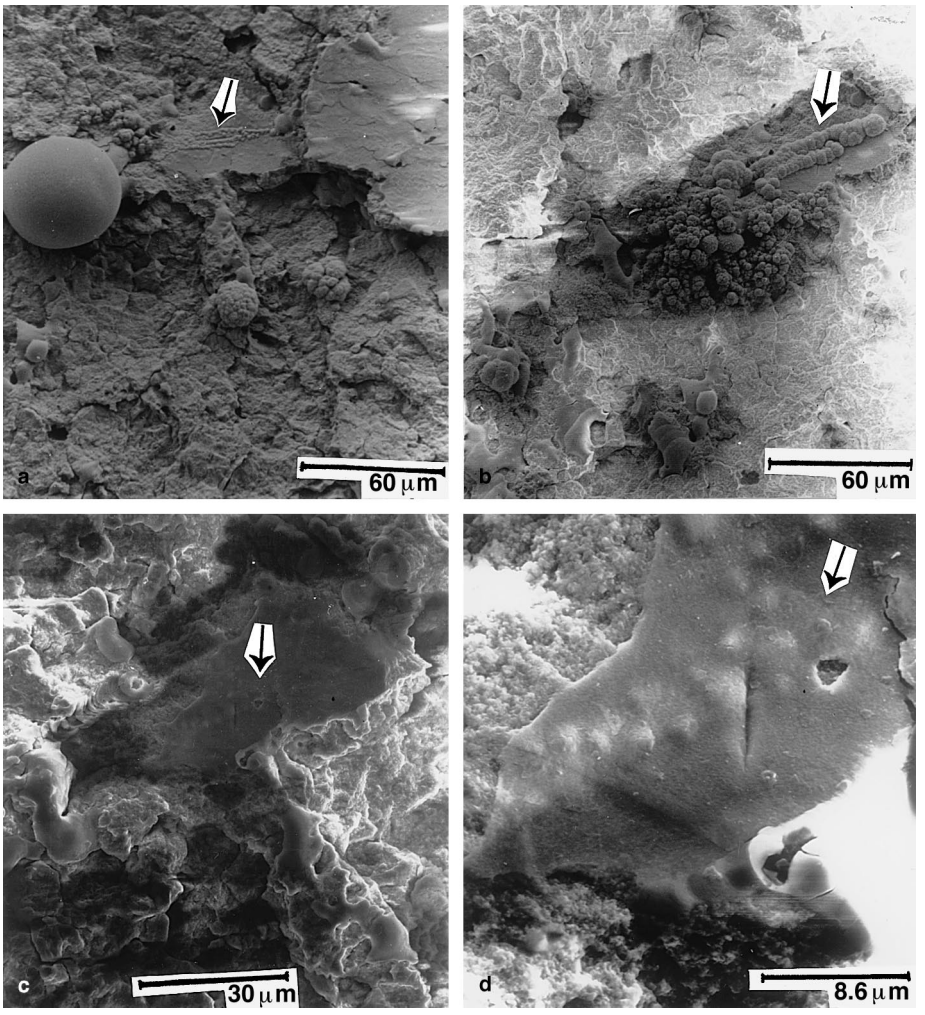

Fig. 4. Cu deposits and their sites on van Arkel zirconium (Be5): (a) First deposit. (b) second deposit. Note that site of large ball in (a) has multiple small Cu particles in (b). (c) Sites arrowed in (b) after removal of Cu deposit. (d) Enlargement of (c).

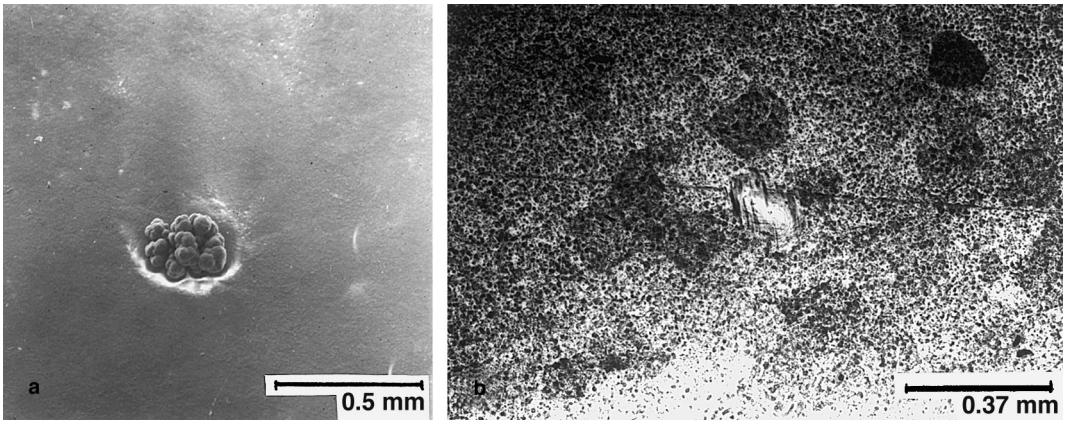

Fig. 5. Cu deposits on Zr–2.5%Nb specimen (Aw265): (a) Low magnification view showing Cu particles. (b) Site after dissolution of Cu (optical micrograph).

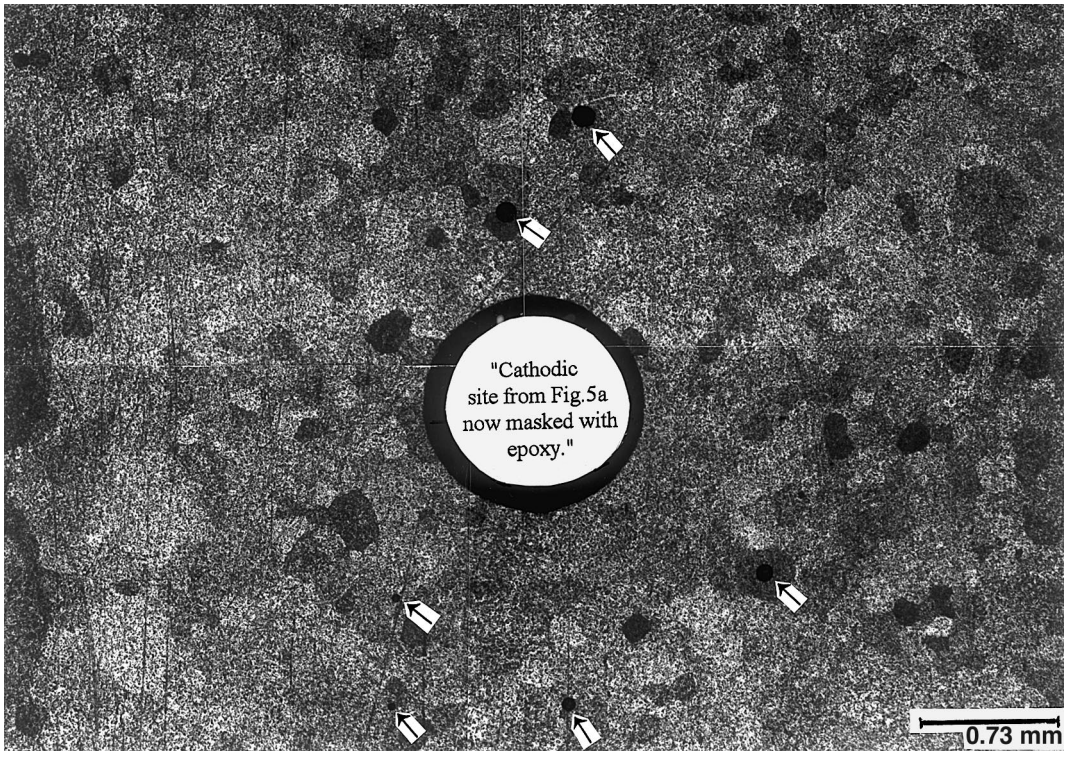

Fig. 6. Minor sites active after major site (shown in Fig. 5) was masked. Arrows indicate Cu deposits (optical micrograph).

taneous oxidation rate [46]. It would appear that this may also be true during pre-transition oxidation, although in this instance, the very small numbers of such sites and their small fractional area may have had insufficient effect on the pre-transition oxidation kinetics to show up in the pressure-change experiments. The whole cathodic current would be able to flow at only a few such sites, whereas the oxide growth process at these

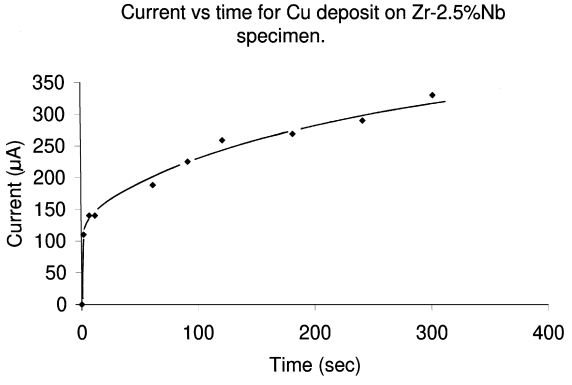

Fig. 7. Increase in cathodic current with time from the start of polarisation.

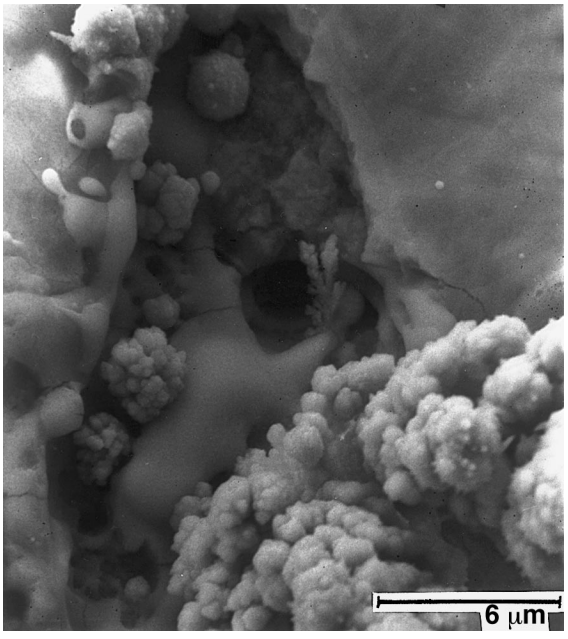

Fig. 8. Cu deposition at carbide particle sites in Zr–2.5%Nb (U16) specimen.

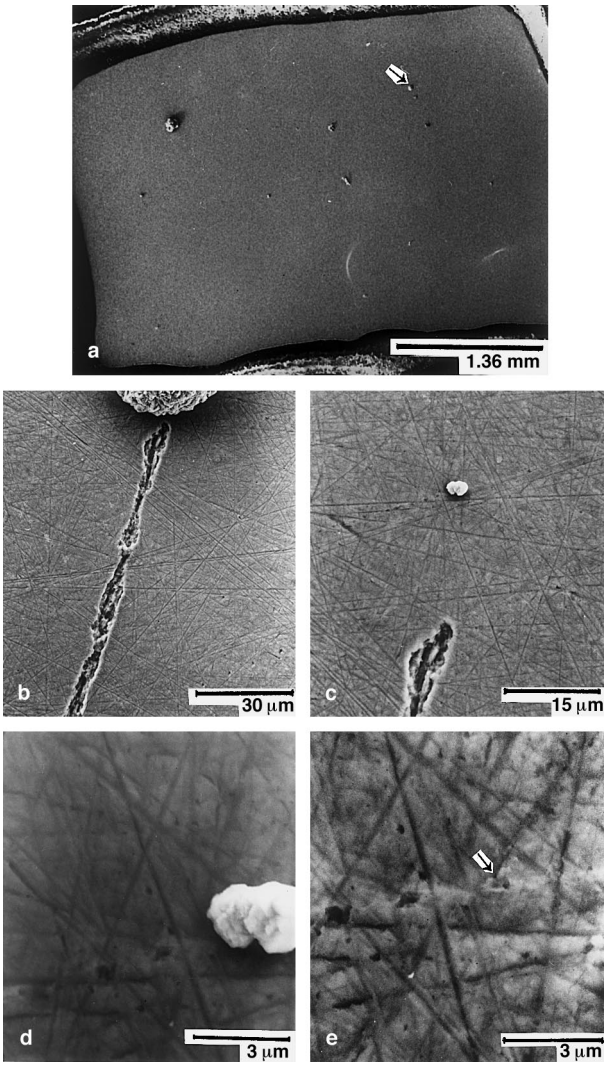

Fig. 9. Distribution of Cu deposits on oxidized Zr–2.5%Nb (PT#790) before (a–e) and after (f–h) degrading in a low pressure hydrogen atmosphere: (a) Specimen C1, first deposit showing distribution of Cu particles. (b) Enlarged view of a Cu particle arrowed in (a). (c) Second Cu deposit with polarization time reduced. (d) Enlarged view of (b). (e) Site after Cu dissolution. (f) Specimen 143A, first deposit showing distribution of Cu particles. (g) Second Cu deposit with polarization time reduced. (h) Sites after Cu dissolution. Arrows locate identical site in each micrograph.

sites would not contribute much to the overall average oxide growth rate. This is in accord with the argument made from changes in hydrogen uptake rate when TSS_H in the matrix is exceeded [9,10]. These changes were found to occur both for pre- and post-transition oxide films (when suitably sized specimens were examined) suggesting that the hydrogen uptake mechanism was the same and was a very localised phenomenon ($\leqslant 10^{-4}$ surface area ratio during post-transition oxidation) during both stages of the oxidation process. The very small cracks identified here as cathodic sites would fit the criteria for such uptake sites.

The large increase in the number of active sites following heating in hydrogen gas, mainly associated with an array of small cracks visible on the surface (Fig. 9), suggests that unlike van Arkel Zr, where small roughly circular pores were generated along prior metal grain boundaries by heating in vacuo, in Zr–2.5%Nb samples heated in hydrogen, it is oxide dissolution at the bottoms of pre-existing (but already passivated) cracks, or the creation of new cracks, in the oxide that creates active cathodic sites. Without stripping the oxides and examining the oxide inner surface (which was not done here), it is not possible to tell whether very

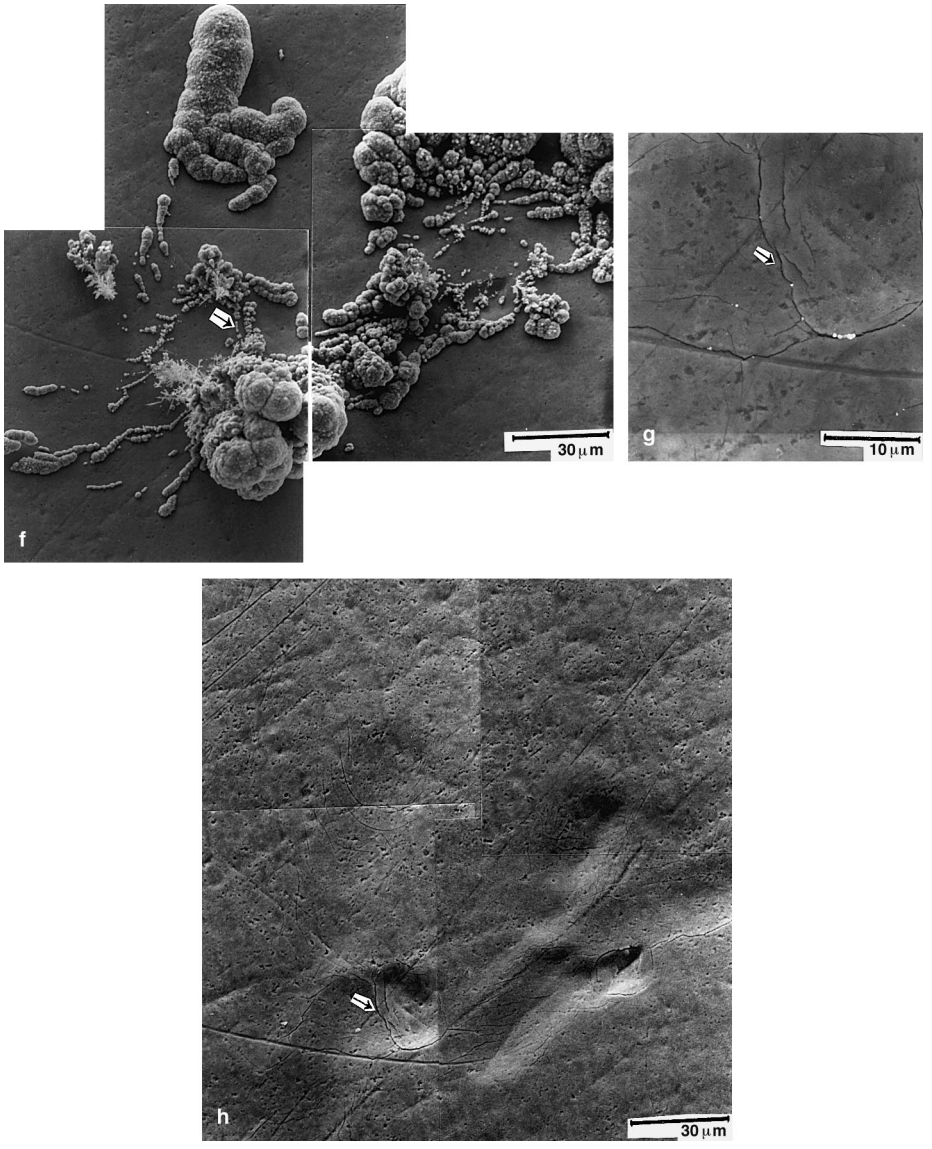

Fig. 9. Cont.

localized oxygen dissolution in the metal was involved in this instance.

The idea that hydrogen uptake during corrosion may be a microscopic version of secondary hydriding by a steam depletion mechanism such as leads to secondary hydriding failures of nuclear fuel cladding [10,47] remains possible, although this study has not resulted in any unequivocal evidence in its favour. When all the evidence is considered, not least the very low (and unmeasured) diffusion coefficients for hydrogen in bulk ZrO_2, it seems to be the micro-mechanism that best fits what we know up to this point, since the occurrence of the cathodic half cell reaction at such sites would rapidly form a small hydrogen bubble [48]. Further evidence that would support this would be observations (by either tritium autoradiography or SIMS) showing that hydride precipitates were being formed at a few sites on the oxide–metal interface once TSS_H was exceeded. The specimens would need to have been rapidly quenched from the corrosion temperature to avoid such segregation happening during slow cooling from the oxidation temperature.

The anomalous conditions observed when large (10 μm) carbide particles were present in the Zr–2.5%Nb alloy is expected to be uncommon, since such particles are not normally present in current production

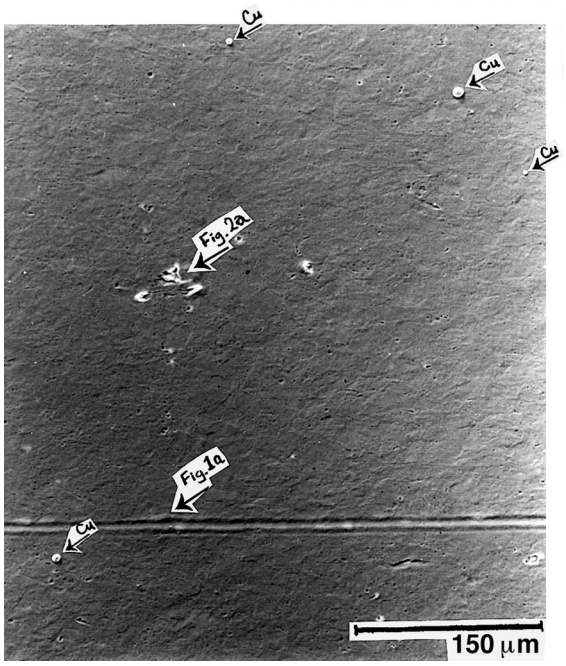

Fig. 10. Area shown in Figs. 1 and 2 (arrows) after a further 1 day oxidation in 400°C steam. New Cu deposit sites also shown by arrows.

Zr–2.5%Nb pressure tubes. The observation of thinner than average oxide over the carbide particles is in line with early work on carbon-melted zirconium, as is the very cracked nature of the oxides formed on such particles [49]. However, even small carbides, which remained undetected in other Zr–2.5%Nb batches may be providing sites for hydrogen ingress. A study of H uptake by Zr–2.5%Nb tubes as a function of carbon content (especially for carbon contents above the carbon solubility of ~100 ppm) could be valuable.

6. Conclusions

The results of the work presented here support an hypothesis that hydrogen uptake during zirconium alloy corrosion is a very localized process. The sites where the cathodic process proceeds had the following characteristics:

- They were invariably locations where cracks or small holes were visible in the oxide.
- They were not associated with intermetallics in the initial specimen surfaces, but pits resulting from intermetallic dissolution during pickling often formed small cracks at their lips that were cathodic sites.
- The sites persisted at room temperature and could be re-decorated, however, even a short oxidation repassivated all previous sites, but generated new ones of similar type.
- In one batch of Zr–2.5%Nb alloy, large (10 μm) carbide particles provided areas of very cracked oxide that were the most active cathodic sites.
- Most batches of Zr–2.5%Nb alloy showed very few cathodic sites, perhaps the cause of their low hydrogen uptake properties.
- Exposure of oxidized Zr–2.5%Nb specimens to a low pressure hydrogen environment generated large numbers of cracks penetrating to the oxide–metal interface that provided extended arrays of cathodic sites rather than the usual discrete sites. Reoxidation rapidly repassivated these. The generation of cracks in

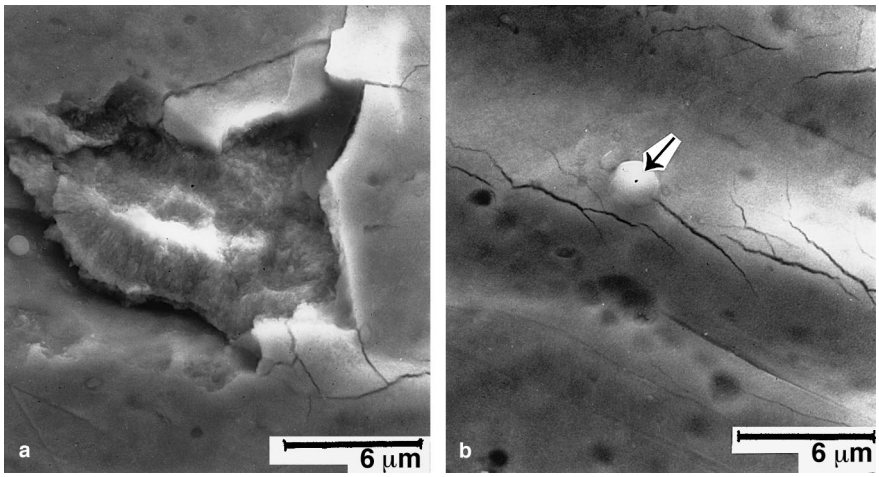

Fig. 11. Details of sites that had previously been active, but were repassivated by heating in 400°C steam: (a) Note small amount of spalling in some places, but no extension of crack patterns at site of scratch in initial surface. (b) Same area as Fig. 1(a) after oxidation. Note very small non-Cu deposit (arrowed) formed during oxidation in steam on the previous cathodic site (1d).

the oxide on Zr–2.5%Nb exposed to hydrogen differs from previous observations of pore generation along prior metal grain boundaries in the oxide on van Arkel Zr.

Acknowledgements

The authors are indebted to the Natural Sciences and Engineering Research Council of Canada, and the CANDU Owners Group for the funds that allowed this study to be performed.

References

[1] K.M. Goldman, D.E. Thomas, Hydrogen pickup during corrosion testing of zirconium, US Report WAPD-MM-184 (February 1953), Bettis Atomic Power Lab., West Mifflin, PA.
[2] A.M. Garde, Enhancement of aqueous corrosion of Zircaloy-4 due to hydride precipitation at the metal/oxide interface, in: Proceedings of 9th Int. Symp. on Zr in the Nuclear Industry, Kobe, Japan, ASTM-STP-1132, 1991, pp. 556–594.
[3] B. Cheng, P.M. Gilmore, H.H. Klepfer, PWR Zircaloy fuel cladding corrosion performance, mechanisms and modelling, in: Proceedings of 11th Int. Symp. on Zr in the Nuclear Industry, Garmisch-Partenkirchen, Ger., ASTM-STP-1295, 1996, pp. 137–160.
[4] R.L. Yang, O. Ozer, H.H. Klepfer, Fuel performance evaluation for EPRI program planning, in: Proceedings of Int. Topical Meeting on LWR Fuel Performance-Fuel for the 90's, Avignon, France, 1991, pp. 258–271.
[5] P. Guedeney, M. Trotabas, M. Boschiero, C. Forat, P. Blanpain, FRAGEMA Fuel Rod Behaviour Characterisation at High Burnup, ibid., 2 (1991) 627–638.
[6] G. Vesterlund, L.V. Corsetti, Recent ABB design and performance experience, in: Proceedings of Internal Topical Meeting on LWR Fuel Performance, W. Palm Beach, FL, 1994, pp. 62–70.
[7] B. Cox, Mechanisms of hydrogen absorption by zirconium alloys, Canadian Report AECL-8702 (1985), Atomic Energy of Canada Ltd., Chalk River Nuclear Laboratories.
[8] B. Cox et al. Waterside corrosion of zirconium alloys in nuclear power reactor, IAEA-TECDOC-996 (1998), International Atomic Energy Agency, Vienna.
[9] B. Cox, J. Alloys Comp. 256 (1997) 244.
[10] B. Cox, J. Nucl. Mater., to be published.
[11] T. Smith, Hydrogen permeation of oxide films on zirconium, US Report NAA-SR-6267 (May 1962), Atomic International, Canoga Park, CA.
[12] T. Smith, J. Electrochem. Soc. 112 (1965) 560.
[13] D.W. Shannon, Corrosion 19 (1963) 414t and U.S. Report HW-76562 Rev. (1963), Hanford Atomic Products Operation, Richland, WA.
[14] T. Smith, J. Nucl. Mater. 18 (1966) 323.
[15] E.A. Gulbransen, K.F. Andrew, J. Electrochem. Soc. 101 (1954) 348.
[16] E.A. Gulbransen, K.F. Andrew, J. Electrochem. Soc. 104 (1957) 709.
[17] S. Aronson, Some experiments on the permeation of hydrogen through oxide films on zirconium, U.S. Report, Bettis Technical Review, WAPD-BT-19 (1960), pp. 75–81, Bettis Atomic Power Lab., W. Mifflin, PA.
[18] J.P. Pemsler, J. Electrochem. Soc. 105 (1958) 315.
[19] K. Une, J. Less Comm. Met. 57 (1978) 93.
[20] W.W. Doerffler, A contribution to the mechanism of dissolution and diffusion of oxygen in zirconium, in: Proceedings of IAEA Conference on Thermodynamics of Nuclear Materials and Atomic Transformations in Solids, Vienna, July 1965, SM66/18; and Swiss Report EIR-82 (1965), Würenlingen, CH.
[21] M. Davis, K.R. Montgomery, J. Standring, J. Inst. Met. 89 (1960) 112.
[22] C.E. Coleman, B. Cox, Cracking zirconium alloys in hydrogen, in: Proceedings of 6th Int. Symp. on Zr in the Nuclear Industry, Vancouver, BC, ASTM-STP-824, 1984, pp. 675–690.
[23] I. Aitchison, D. Khatamian, J. den Hartog, Z. Phys. Chem. 181 (1993) 441.
[24] N.S. McIntyre, R.D. Davidson, C.G. Eisener, G.M. Good, G.R. Mount, B.D. Warr, M. Elmoselhi, J. Vac, Sci. Technol. A 9 (1991) 1402.
[25] M.B. Elmoselhi, J. Alloys Comp. 231 (1995) 716.
[26] C. Roy, Hydrogen distribution in oxidised zirconium alloys by autoradiography, Canadian Report, AECL-2085 (1964), Atomic Energy of Canada Ltd., Chalk River Nuclear Laboratories.
[27] J.P. Butler, The determination of deuterium in the surface layers of D_2O-oxidised Zircaloy-2 by the D (d,n) He^3 Reaction, in: Proceedings of IAEA Conference on Radiochemical Methods of Analysis, vol. 1, Vienna, 1965, pp. 391–403.
[28] B.F. Kammenzind, D.G. Franklin, H.R. Peters, W.J. Duffin, Hydrogen pickup and redistribution in alpha-annealed Zircaloy-4, in: Proceedings of 11th Int. Symp. on Zr in the Nuclear Industry, Garmisch-Partenkirchen, Ger., ASTM-STP-1295, 1996, pp. 338–370.
[29] B. Cox, N. Ramasubramanian, V.C. Ling, Zircaloy Corrosion Properties Under LWR Coolant Conditions, Part 1, Electric Power Research Inst. Report NP6979-D, 1990.
[30] M.B. Elmoselhi, B.D. Warr, S. McIntyre, A study of the hydrogen uptake mechanism in zirconium alloys, in: Proceedings of 10th Int. Symp. on Zr in the Nuclear Industry, Baltimore, MD., ASTM-STP-1245, 1994, pp. 62–79.
[31] N. Ramasubramanian, Lithium and boron effects in the corrosion mechanism of zirconium alloys under coolant chemistry conditions, in: Proceedings of 7th Int. Conf. on Water Chemistry of Nuclear Reactor Systems, Bournemouth, vol. 1, UK, 1996, pp. 91–93, .
[32] D. Khatamian, Z. Phys. Chem. 181 (1993) 435.
[33] D. Khatamian, J. Alloys Comp. 253&254 (1997) 471.
[34] B. Cox, J.A. Read, Oxidation of a Zr–2.5%Nb Alloy in steam and air, UK Report, AERE-R4459 (1963), UK Atomic Energy Authority, Harwell, Berks.
[35] B. Cox, T. Johnston, Trans. Met. Soc. AIME 227 (1963) 36.
[36] B. Cox, H.I. Sheikh, J. Nucl. Mater. 249 (1997) 17, and unpublished results.

[37] B. Cox, M.J. Davis, A.D. Dent, The oxidation and corrosion of zirconium and its alloys, Part X, Hydrogen absorption during oxidation in steam and aqueous solutions, UK Report, AERE-M621 (April 1960), UK Atomic Energy Authority, Harwell, Berks.
[38] B. Cox, The effect of some alloying additions on the oxidation of zirconium in steam, UK Report, AERE-R4458 (September 1963), UK Atomic Energy Authority, Harwell, Berks.
[39] B. Cox, Zirconium intermetallics and hydrogen uptake during corrosion, Canadian Report, AECL-9383 (April 1987), Atomic Energy of Canada Ltd., Chalk River Nuclear Labs.
[40] Y. Hatano, K. Isobe, R. Hitaka, M. Sugisaki, J. Nucl. Sci. Tech. 33 (1996) 944.
[41] K. Isobe, Y. Hatano, M. Sugisaki, J. Nucl. Mater. 248 (1997) 315.
[42] F. Lefebvre, CEA, Grenoble, France, private communication.
[43] I. Takagi, T. Hattori, M. Hashizumi, K. Higashi, Nucl. Instrum. Meth. B 118 (1996) 238.
[44] B. Cox, F. Gauducheau, Y.M. Wong, J. Nucl. Mater. 189 (1992) 362.
[45] B. Cox, A.R. McIntosh, The oxide topography on crystal-bar and reactor grade sponge zirconium, Canadian Report, AECL-3223 (1968).
[46] B. Cox, J. Less Common Met. 5 (1963) 325.
[47] R.L. Yang, O. Ozer, S.K. Yagnik, B. Cheng, H.H. Klepfer, H. Kjaer-Pederson, P. Rank, EPRI Failed fuel degradation R&D program, in: Proceedings of 1994 Int. Top Meeting on Light Water Reactor Fuel Performance, W. Palm Beach, FL, 435–446.
[48] B. Cox, What is wrong with current models for in-reactor corrosion, in: Proceedings of IAEA Technical Committee. Meeting on Fundamental Aspects of Corrosion on Zirconium Base Alloys in Water-Reactor Environments, IWGFPT/34, Portland, OR, September 1989, pp. 167–173.
[49] B. Cox, Corrosion 16 (1960) 188t.
[50] Y-P. Lin, Nature of oxidised β-phases in the Zr–2.5 Nb alloy, in: Proceedings of 3rd Int. Conf. on Microscopy of Oxidation, Cambridge, UK, 1996.